Probing Actin and Liposome Interaction of Talin and Talin–Vinculin Complexes: A Kinetic, Thermodynamic and Lipid Labeling Study†

W. H. Goldmann,‡ V. Niggli,§ S. Kaufmann,‡ and G. Isenberg*,‡

Biophysics Department, E22, Technical University of Munich, D-8046 Garching, FRG, and Department of Pathology, University of Bern, CH-3010 Bern, Switzerland

Received January 2, 1992

ABSTRACT: Talin purified from human platelets and chicken gizzard smooth muscle is an actin and lipid binding protein. Here, we have investigated the effect of vinculin on (a) talin-nucleated actin polymerization and (b) insertion of talin into lipid bilayers. Calorimetric data show ternary complex formation between talin, vinculin, and actin. Actin–talin, actin–vinculin and actin–(talin–vinculin) binding and rate constants as well as actin polymerization rates for all three protein species have been determined by steady state titration, stopped-flow, and fluorescence assay. In contrast to an increase of the polymerization rate by a factor of <2 for actin–talin and actin–(talin–vinculin) when lowering the temperature, we measured a decrease in rates for actin alone and actin–vinculin. The overall equilibrium constants (K_{eq}) in the van't Hoff plot proved linear and were of one-step reactions. Thermodynamic data exhibited signs of van der Waal's binding forces. Using the photoactivatable lipid analogue [^{3}H]PTPC/11, which selectively labels membrane-embedded hydrophobic domains of proteins, we also show that talin partially inserts into the hydrophobic bilayer of liposomes. This insertion occurs in a similar manner irrespective of preincubation with vinculin.

We believe that talin is a key protein mediating the anchorage of the microfilament system to plasma membranes serving a dual function as a nucleating protein for actin filament assembly at the membrane interface (Isenberg, 1991).

This hypothesis is based on the recent finding that talin can be reconstituted into liposomes where it preferentially interacts with charged phospholipids as demonstrated by differential scanning calorimetry (DSC) and Fourier transformed infrared spectroscopy (FTIR) (Heise et al., 1991). On the other hand, it was recently shown that talin binds to actin (Muguruma et al., 1990; Goldmann & Isenberg, 1991) as it was assumed by Collier & Wang (1982) and further acts as a nucleation-promoting protein for actin filament polymerization in vitro (Kaufmann et al., 1991).

It is these two features, (a) membrane anchorage and (b) actin polymerization-promoting activity, which one would have anticipated simply from the correlation of the fluorescent localization of talin with growing actin bundles in the outer periphery of leading lamellae in locomoting fibroblasts (Izzard, 1988; Hock et al., 1989; De Pasquale & Izzard, 1991).

Recent evidence shows that vinculin assembles into these talin/actin-rich precursor structures at the membrane interface (Izzard, 1988; De Pasquale & Izzard, 1991; Feltkamp et al., 1991) before these gradually develop into the more complex adhesion plaques or focal contact, where both proteins, vinculin and talin, initially have been colocalized [for reviews, see Geiger et al. (1987); Burridge et al. (1988); Beckerle and Yeh (1990); and Turner and Burridge (1991)].

In our attempt to reconstitute cytoskeleton membrane assembly structures (CYMAS) in vitro, it was of interest to investigate what effect the addition of just one more component, namely, vinculin, would have on (a) talin–actin interaction and (b) the insertion of talin into liposomal membranes.

MATERIALS AND METHODS

Reagents. G buffer: 2 mM Tris-HCl, pH 8.0, 0.2 mM $CaCl_2$, 0.2 mM ATP, 0.2 mM DTT, and 0.005% NaN_3 used in steady-state and stopped-flow studies. F buffer: 2 mM Tris-HCl, pH 8.0, 0.2 mM $MgCl_2$, 100 mM KCl, 0.2 mM $CaCl_2$, 0.5 mM ATP, 0.2 mM DTT, and 0.005% NaN_3 used in polymerization studies.

Phosphatidylserine was obtained from Lipid Products, South Nutfield, Surrey, England. [^{3}H]PTPC/11[1] was prepared as described previously (Harter et al., 1988) with a specific activity of 15 Ci/mmol. All reagents were of the highest purity available.

Proteins. Actin was prepared according to Spudich and Watt (1971) from acetone powder obtained from rabbit back muscle followed by a gel filtration step as described by MacLean-Fletcher and Pollard (1980). Fractionated G-actin beyond the elution peak (at ~1 mg/mL) was stored in G buffer at 4 °C. G-Actin was labeled with 7-chloro-4-nitrobenzeno-2-oxa-1,3-diazole (NBD) for fluorescence measurements following the protocol of Detmers et al. (1981).

Platelet talin and vinculin were isolated from outdated (not older than 10 days) human thrombocytes by the Collier and Wang (1982) method. Talin was further purified by passing it through a gel filtration column (Kaufmann et al., 1991). After the first ionic-exchange column according to this protocol, vinculin was purified by an additional hydroxylapatite column and eluted by a linear gradient from 0.02 to 0.4 M KH_2PO_4.

† Supported by DFG Grants Is 25/5-2 and SFB 266 C-5 and by the Swiss National Foundation for Scientific Research.

* Address correspondence to this author.

‡ Technical University of Munich.

§ University of Bern.

[1] Abbreviations: EGTA, ethylene glycol bis(β-aminoethyl ether)-*N,N,N',N'*-tetraacetic acid; HEPES *N*-(2-hydroxylethyl)piperazine-*N'*-2-ethanesulfonic acid; [^{3}H]PTPC/11, 1-palmitoyl-2-[11-[4-[3-(trifluoromethyl)diazirinyl]phenyl][2-^{3}H]undecanoyl]-*sn*-glycero-3-phosphocholine; NBD, 7-chloro-4-nitrobenzeno-2-oxa-1,3-diazole; SDS, sodium dodecyl sulfate.

0006-2960/92/0431-7665$03.00/0

Chicken gizzard smooth muscle talin and vinculin were isolated by the O'Halloran et al. (1986) method. After the first purification step (DE 52 column), vinculin was purified by a hydroxylapatite column as in the platelet preparation.

The purity of the proteins was analyzed on SDS minislab gels. Protein concentrations were determined according to Bradford (1976).

Rat IgG was isolated from rat whole serum (Zymed, San Francisco, CA) using an Affi-Prep Protein A kit (Bio-Rad, Richmond, CA).

Equilibrium Binding and Polymerization Experiments. Fluorescence measurements taken at a 90° angle were carried out on a Spex Fluorolog 1680 0.22 double spectrophotometer. The cell holder was thermostatically temperature controlled by an external water bath with a temperature control of ±0.1 °C. Normally, a 3-mL four-sided quartz cuvette of 1 cm path length was used for equilibrium measurements. For polymerization experiments, a 1-mL four-sided quartz cuvette was employed. Proteins and reagents were added and gently stirred by hand to prevent the formation of air bubbles. In equilibrium binding studies, the sample was continuously stirred by a magnetic flea. NBD–actin fluorescence was recorded by exciting at 480 nm and emitting at 530 nm with a band pass width of 2 nm. Kinetic data were collected on a Spex computer (program DM3000) and printed on a Mannesmann tally chart printer.

Calorimetric Experiments. Measurements were performed on a high-sensitivity differential scanning microcalorimeter supplied by Microcal (Amherst, MA). Data storage and analysis were carried out on an IBM AT computer using DA-2 software also provided by Microcal. Before each experiment, the samples were precooled on ice. The heating scan was started after 20 min of temperature equilibrium at a rate of 90 °C/h with a 15-s time increment between each data collection.

Stopped-Flow Experiments. The rapid-mixing studies were performed at ambient temperature on a stopped-flow spectrophotometer Model 1705 supplied by Applied Photophysics Ltd. (Leatherhead, England). The dead time of the apparatus is approx. 2 ms as stated by the suppliers. The optical system consisted of a 30-W Xenon lamp with a monochromator set at 480 nm and a slit width of 2 nm. The light was transmitted to the integral mixing and observation chamber by a direct light path. For fluorescence measurements, the 90° emitted light was detected by a 1P28-type photomultiplier via a quartz light guide. The signal from the photomultiplier was captured by a Commodore XT computer and analyzed on a commercially available Macintosh LC computer program (IGOR).

Preparation of [^{3}H]PTPC/11-Containing Liposomes. A mixture of phosphatidylserine and [^{3}H]PTPC/11 (0.3% w/w of total lipid) in chloroform–methanol (2:1) was evaporated under N_2, and the phospholipid film was dried under vacuum for 30 min at room temperature. The phospholipid was then dispersed by sonication in a buffer containing 20 mM Hepes and 0.2 mM EGTA, pH 7.4 (1 mg of lipid/mL). Sonication was performed under N_2 in a bath sonifier (Laboratory Supplies Co., Hicksville, NY, Model G112SPIT). The clear dispersions were centrifuged at 100000*g* for 30 min at 4 °C to pellet multilamellar liposomes. The supernatant containing small unilamellar liposomes was used for labeling the same day.

Photolysis. Prior to experimentation, talin and vinculin were dialyzed against buffer C (20 mM Tris-HCl, pH 7.4, 0.1 mM EDTA, 15 mM 2-mercaptoethanol). After centrifugation in an Eppendorf centrifuge (10 min), the protein content of the supernatant was determined (Bradford, 1976), using bovine serum albumin as the standard. Protein determination according to Lowry et al. (1951) with bovine serum albumin as the standard gave the same results.

Talin was incubated at room temperature with the liposomes in the presence and absence of vinculin under the conditions indicated in the figure legend. Buffer C was added to a final volume of 200 μL. As a control for a soluble protein, rat IgG [30 μg/200 μL as determined by Lowry et al. (1951) with bovine serum albumin as the standard] was incubated with liposomes under the same conditions as talin in the absence of mercaptoethanol. In some experiments, 130 mM KCl and 1 mM $MgCl_2$ (final concentrations) were present in the incubation medium. The samples were transferred to a quartz cuvette and photolyzed for 4 min, using a mercury lamp (HBO 200, Wild) with a saturated solution of copper sulfate (20 mm) as a filter.

SDS–Polyacrylamide Gel Electrophoresis and Autoradiography. After photolysis, a threefold concentrated sample buffer was added to the protein–lipid mixtures to yield a final concentration of 2.5% SDS, 50 mM dithiothreitol, 15% (v/v) glycerol, 62.5 mM Tris, pH 6.8, and 0.001% bromphenol blue. Extraction of the samples with chloroform–methanol prior to electrophoresis—in order to extract noncovalently bound lipid (Niggli et al., 1986)—was omitted as this treatment led to a low recovery of talin. Direct application of lipid–protein mixtures to the gel did not result in unspecific binding of lipids to protein as nonphotolyzed controls did not contain significant amounts of label (see Results). The samples were incubated for 5 min at 95 °C and subsequently applied to 5–20% SDS–polyacrylamide gradient gels (Laemmli, 1970). The gels were then fixed for 30 min in 45% (v/v) methanol and 1% (v/v) acetic acid followed by several washes in H_2O and in 50 mM Tris-HCl, pH 7. Staining with Coomassie Blue was omitted at this stage as this dye reduces the signal. Finally, the gels were incubated for 30 min in 1 M sodium salicylate at pH 6 (Chamberlain, 1979), dried under vacuum/heat, and exposed to a preflashed (Laskey & Mills, 1975) Kodak X-AR 5 film at −70 °C. After autoradiography the gels were rehydrated and stained with Coomassie Blue.

Quantitative Evaluation of Labeling. Protein-containing slices were cut out from Coomassie Blue-stained 5–10% gradient gels (Niggli et al., 1986) together with slices from the same lane in protein-free areas for evaluation of background. The slices were incubated with 0.6 mL of NCS solubilizer (Amersham, Buckinghamshire, U.K.) and 60 μL of H_2O in glass scintillation vials for 2 h at 50 °C. After cooling to room temperature, 3.5 mL of Instagel (Packard) was added to the slices. After incubation for 16 h in the dark, the vials were counted in a Kontron BETAmatic I liquid scintillation counter. Background counts per minute obtained in the same lane were substracted from the counts per minute extracted from the protein bands. The degree of quenching of radioactivity due to NCS solubilizer was evaluated by adding defined amounts of [^{3}H]PTPC/11 to Coomassie Blue-stained gel slices incubated in NCS solubilizer. This procedure reduced the counts per minute measured by approximately 35%. To correct for unequal protein loading, the amount of protein in the bands was evaluated by scanning the Coomassie Blue-stained gels and was compared with defined amounts of talin and vinculin. Staining intensity was linear in the range of 2–8 μg of protein.

RESULTS

Figure 1 shows the purified proteins, talin, vinculin, and actin, used in our experiments.

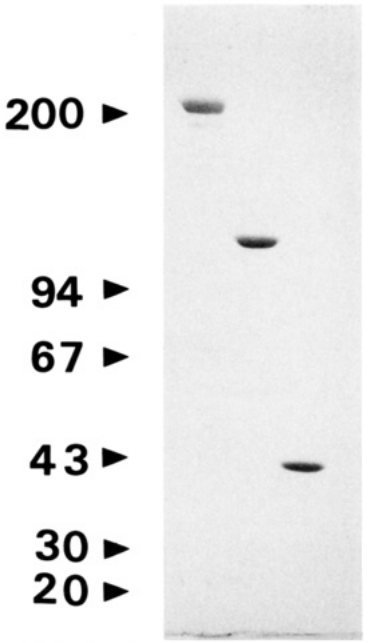

FIGURE 1: 5–10% SDS–polyacrylamide gradient gel showing the purified proteins: talin (lane 1), vinculin (lane 2), and actin (lane 3). MW standards are indicated by numbers; 5 μg of protein was loaded per lane.

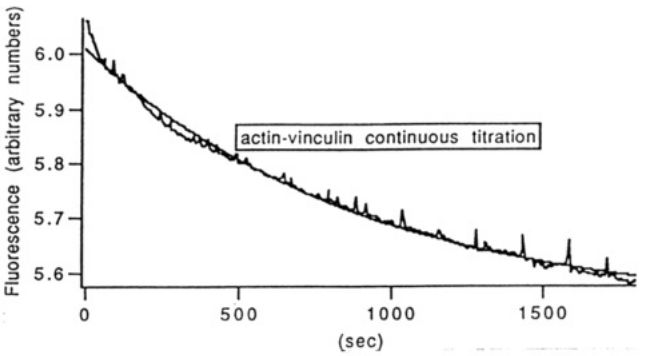

FIGURE 2: Continuous titration of 0.14 mg/mL of vinculin at a rate of 70 μL/min into a 3-mL cuvette containing 0.025 mg/mL of ~100% NBD labeled G-actin. Buffer conditions: 5 mM Tris-HCl, 0.2 mM DTT, 0.2 mM $CaCl_2$, and 0.5 mM ATP, pH 8.0, at 25 °C.

Equilibrium Binding and Polymerization Studies. The use of NBD fluorescence label on G-actin allows continuous titration in order to determine the affinity, of talin, talin–vinculin, or vinculin for G-actin. As an example, actin–vinculin titration is shown in Figure 2. For this kind of titration studies G-actin was labeled to approximately 100% with 7-chloro-4-nitrobenzeno-2-oxa-1,3-diazole (NBD) to ensure a high signal to noise ratio in comparison with only 5% labeling, which gave similar binding constants. All traces were fitted by using a nonlinear least-squares fitting routine (Goldmann & Isenberg, 1991).

The value of the overall equilibrium constant (K_{eq}) obtained from these titrations in Table I compares with previous estimates (Goldmann et al., 1991), indicating that an increase in temperature leads to a decrease of the overall K_{eq} by a factor of 2–3 over a 20 °C temperature range. The thermodynamic data calculated from the van't Hoff plot using these equilibrium constants are presented in Table II.

For all three binding species, the enthalpy ($\Delta H°$) remains relatively constant varying from –46.2 to –27.6 kJ/mol, showing that the principal reaction mechanism does not change. The negative values for $\Delta G°$ are indicative that G-actin favors protein association with talin, talin–vinculin, and vinculin. The negative values for both $\Delta H°$ and $\Delta S°$ are characteristic for nonbonded (van der Waals) interaction, hydrogen bond formation, and/or protonation associated with protein binding. Since we did not see any significant difference in binding affinity for all protein–protein interactions in the presence of vinculin (Table I), we have, in addition, investigated the effect of vinculin on the polymerization rate of actin in the presence and absence of talin. In a typical polymerization experiment 4.5 μM G-actin (5% NBD–actin and 95% unlabeled actin) was mixed with F buffer with either talin, talin–vinculin, or vinculin at the same total protein concentration (Figure 3A–D). The rate of polymerization monitored by change of fluorescence signal for these reactions was calculated by using the following equation:

$$k = ln\ 2/t_{1/2}$$

where ln 2 is the natural logarithmic of 2; $t_{1/2}$ is the time elapsed after half-maximal polymerization amplitude, and k is the rate (in s^{-1}). The data in Table III, obtained by using this method at various temperatures, showed that (a) the polymerization rates for actin–talin and actin–(talin–vinculin) (at a 1:1 molar ratio) were almost identical and (b) the polymerization rates for actin in the presence and absence of vinculin were very similar. This result supports the notion that vinculin has a negligible effect on actin–talin binding and talin-induced actin polymerization. Furthermore, it is of interest that the polymerization rates of actin–talin and actin–(talin–vinculin) increase when lowering the temperature by

Table I: Equilibrium Constants (K_{eq}) × 10^6 M^{-1}[a]

	5 °C	10 °C	15 °C	20 °C	25 °C
G-actin–talin	5.0	3.5	3.3	3.2	1.5
G-actin–talin–vinculin	4.7	3.0	2.8	2.5	1.4
G-actin–vinculin	3.1	2.5	2.1	1.9	1.6

[a] Equilibrium constants were obtained by fluorescence continuous titration in G buffer. G-Actin concentrations were near the overall binding constant (K_d).

Table II: Thermodynamic Data Deduced from van't Hoff Plot of Variation of Equilibrium Constants (Table I) with Temperature[a]

	$\Delta H°$, kJ mol^{-1}	$\Delta G°$, kJ mol^{-1}	$\Delta S°$, J mol K^{-1}
G-actin–talin	–46.2	–35.7	–36
G-actin–talin–vinculin	–42.5	–34.9	–26
G-actin–vinculin	–27.6	–35.3	–26

[a] The thermodynamic data were calculated using the following equations:

$$\log (K_2/K_1) = \Delta H°(T_2 - T_1)/2.303RT_1T_2 \quad (1)$$

$$\Delta G° = -RT \ln K \quad (2)$$

$$\Delta G° = \Delta H° - T\Delta S° \quad (3)$$

with the following values for the constants: R (gas constant) = 8.31 J K^{-1} mol^{-1} and T (absolute temperature) in Kelvin.

Table III: Polymerization Rates (s^{-1}) × 10^{-3} [a]

	5 °C	20 °C	35 °C
(1) G-actin	~0.40	~1.60	~1.90
(2) G-actin–vinculin	~0.44	~1.50	~1.60
(3) G-actin–talin	~5.10	~4.10	~3.50
(4) G-actin–talin–vinculin	~4.90	~4.00	~3.30

[a] Fluorescence change of 5% NBD–actin and 95% unlabeled actin at various temperatures. (1) 4, 5 μM actin only; (2) 4, 5 μM actin and 1, 5 μM vinculin; (3) 4, 5 μM actin and 1, 5 μM talin; (4) 4, 5 μM actin, and 1, 5 μM talin, and 1, 5 μM vinculin. Polymerization was started by addition of F buffer to the above solutions.

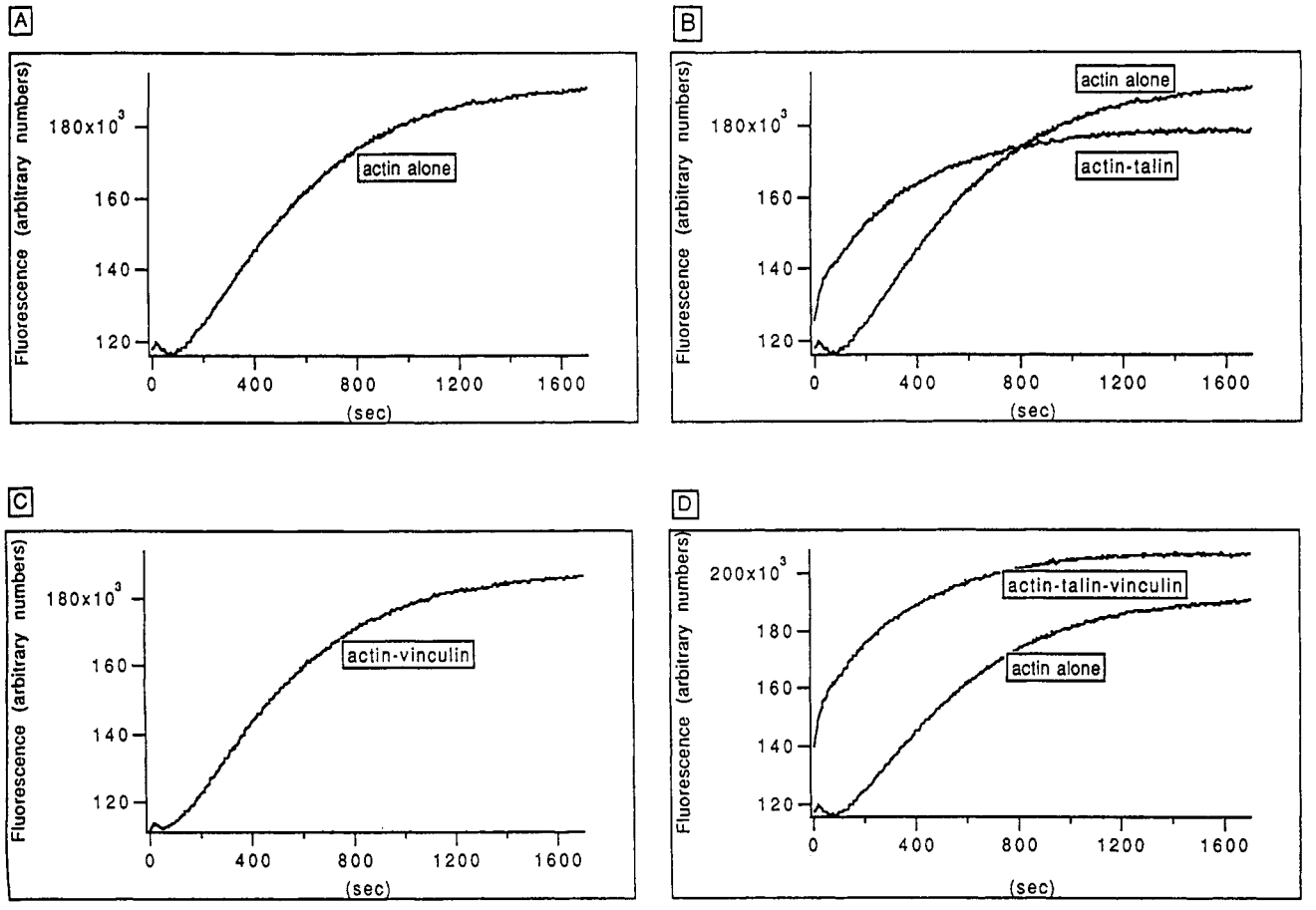

FIGURE 3: Fluorescent traces of 4.5 μM 5% NBD–actin and 95% unlabeled actin polymerizing in F buffer (A); in the presence of 1.5 μM talin (B); in the presence of 1.5 μM vinculin (C); in the presence of 1.5 μM talin and 1.5 μM vinculin (D). All experiments were carried out at 20 °C.

a factor of <2 while the rates for actin alone and actin–vinculin decrease by a factor >2.

Calorimetric Studies. Calorimetric measurements have been reported to provide an effective method for establishing direct evidence of protein–protein interaction (Ross & Subramaian, 1981). We have used this technique to assay ternary complex formation between G-actin, talin, and vinculin. In order to verify the assumption that G-actin alone (A) and G-actin when bound to talin (B), vinculin (C), and talin–vinculin (D) exhibit different temperature dependence of protein unfolding, we scanned all species from 20 to 90 °C. Figure 4 shows that the specific heat capacity (C_p) of all traces is similar between 20 and 40 °C. However, a further increase in temperature up to 90 °C resulted in a decrease of C_p values (traces A→D), which correlate with actin–vinculin, actin–talin, and actin–vinculin–talin binding. This result is indicative of strong intra- and/or intermolecular forces connected with protein binding (Goldmann & Isenberg, 1992) and supports the interpretation of the thermodynamic data calculated from the van't Hoff plot (Goldmann et al., 1991).

Stopped-Flow Studies. The association rate constants were obtained by stopped-flow technique. NBD–G-actin was mixed with talin, talin preincubated with vinculin (at a 1:1 molar ratio), or vinculin. The fluorescence decay could be described by a single exponential for all protein species. Figure 5 shows a typical result of a least-squares fit exponential superimposed. Assuming an overall binding mechanism

$$A + B \underset{k_{-1}}{\overset{k_{+1}}{\rightleftarrows}} AB$$

where A is actin and B is talin, talin–vinculin, or vinculin, the observed rate of fluorescence change is given by the following equation:

$$1/\tau = k_{+1}([A] + [B]) + k_{-1}$$

The kinetic data obtained from these experiments are presented in Table IV together with the calculated "off"-rates deduced from the overall $K_{eq} = k_{+1}/k_{-1}$ (Table I). The observed association rate constant for G-actin–talin binding compares with published data. However, there are reasons for believing the mechanism for all reactions is more complex (Goldmann & Isenberg, 1991). So far, we have not yet been able to determine individual binding and rate constants based on the reported stoichiometries. The small change in the association rate constant noted here reflects similar changes in the overall K_{eq} and polymerization rates, again indicating a negligible effect of vinculin on G-actin–talin binding.

Lipid Photolabeling. Membrane insertion of talin was probed by a photoactivatable lipid analogue. As shown in Figure 6, talin incorporated substantial amounts of label upon incubation and photolysis with phosphatidylserine liposomes containing trace amounts of the photoactivatable phospholipid [^{3}H]PTPC/11. Talin incorporated 1190 ± 490 (mean ±SD of n = 4 independent experiments) cpm per 5 μg of protein when incubated with liposomes in the absence of added KCl and $MgCl_2$ (Figure 6, lane 6). Vinculin under the same conditions incorporated comparable amounts of label (1060 ± 270 cpm, n = 4). Specific labeling of talin and vinculin corresponds to 0.004–0.01 mol of label/mol of protein and 0.002–0.003 mol of label/mol of protein, respectively, after correction for quenching (see Materials and Methods). Talin incorporated 0.1–0.3% and vinculin 0.1–0.2% of total label.

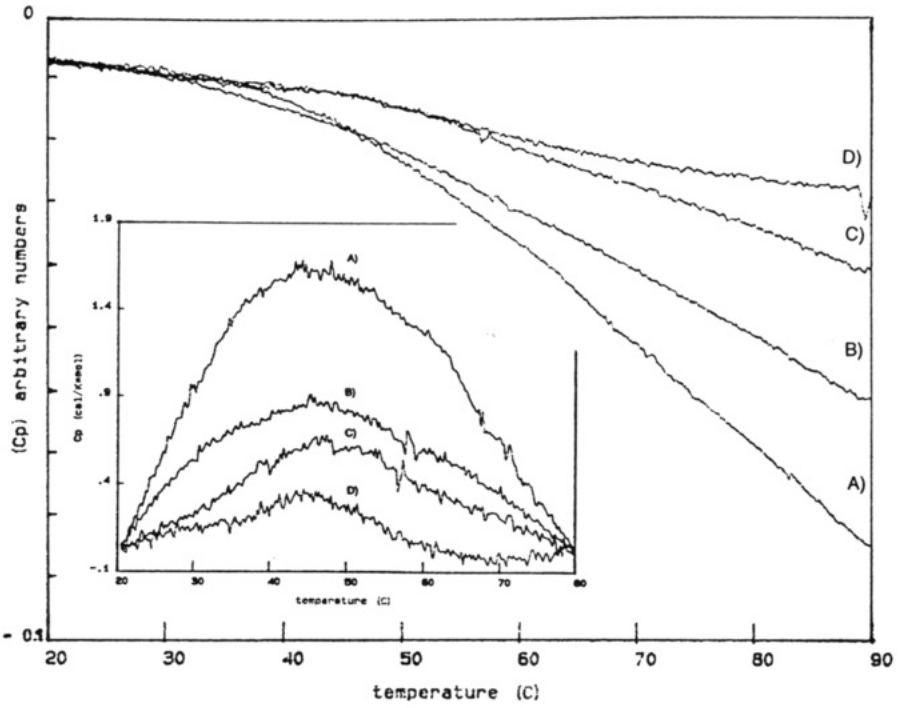

FIGURE 4: The traces (A–D) demonstrate changes in specific heat capacity (C_p) of unfolding proteins with increasing temperature. (Inset) Scans (A–D) are normalized after deduction of G buffer baseline. All experiments were performed in G buffer at a total protein concentration of 5 μM. Molar ratio of actin:talin is 3:1 and of talin:vinculin is 1:1.

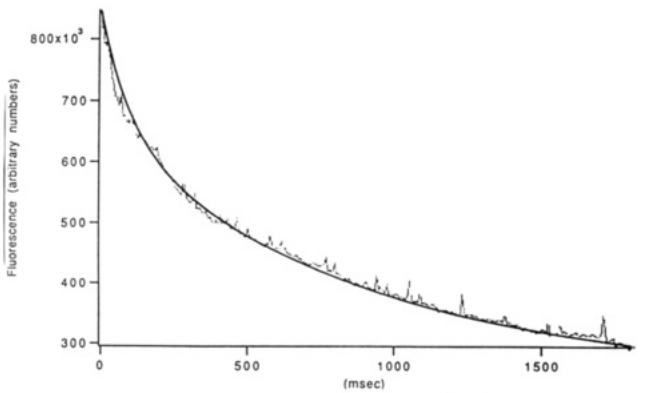

FIGURE 5: Trace represents an average of three consecutive measurements at ambient temperature in the stopped-flow apparatus. The best fit to a single exponential is shown superimposed. Buffer conditions are as in Figure 2. Protein concentration: 0.75 μM G-actin labeled to ~100% with NBD and 0.5 μM vinculin. The observed rate $1/\tau = 2.75\ s^{-1}$.

Table IV: Association and Dissociation Rate Constants[a]

	$k_{+1} \times 10^6$, $M^{-1}\ s^{-1}$ (measd)	k_{-1}, s^{-1} (calcd)
G-actin–talin	4, 3 (±0, 8; 6)	~1, 3
G-actin–talin–vinculin	2, 8 (±1, 2; 6)	~1, 1
G-actin–vinculin	2, 2 (±1, 1; 5)	~1, 2

[a] Association rate constants were obtained in G buffer from stopped-flow experiments. Dissociation rate constants were determined from the relation overall $K_{eq} = k_{+1}/k_{-1}$. Numbers in parentheses give the standard deviation and number of observations, respectively.

For comparison, transmembrane protein glycophorin A incorporated 0.2–0.4% (Brunner et al., 1983). The relatively low labeling efficiency obtained with carbene-generating photoactivatable reagents is due to a predominant reaction of the highly reactive intermediates with phospholipids (Brunner, 1989). For control, isolated rat IgG was incubated with [^{3}H]-PTPC/11 phosphatidylserine liposomes under the same

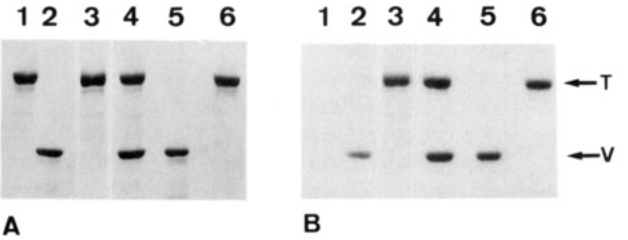

FIGURE 6: Hydrophobic photolabeling of talin upon incubation with phosphatidylserine liposomes containing trace amounts of a photoactivatable phospholipid. Talin alone or mixtures of talin and vinculin were preincubated in the absence of liposomes for 15 min at room temperature. Phosphatidylserine liposomes containing trace amounts of [^{3}H]PTPC/11 were then added to the proteins, and incubation was continued for a further 15 min. Final concentration of the lipid was 0.5 mg/mL and of protein was 0.15 mg/mL (30 μg of a single protein, or 15 μg per protein for combinations of two proteins per 200 μL). Subsequently, the samples were photolyzed and analyzed by SDS–gel electrophoresis and autoradiography (see Materials and Methods). 5 μg of protein (10 μg of combinations) was applied per lane. (a) Coomassie Blue-stained 5–20% gradient gel; (B) The corresponding autoradiogram. (Lane 1) talin incubated with liposomes without photolysis; (lane 2) vinculin incubated with liposomes in the presence of 130 mM KCl and 1 mM $MgCl_2$; (lane 3) talin incubated with liposomes in the presence of 130 mM KCl and 1 mM $MgCl_2$; (lane 4) talin and vinculin, incubated with liposomes in the absence of added salt; (lane 5) vinculin incubated with liposomes in the absence of added salt; (lane 6) talin incubated with liposomes in the absence of added salt. Arrows on the right indicate the position of talin (T) and vinculin (V).

conditions as described for talin (legend of Figure 6, without addition of salt). IgG incorporated tenfold less radioactivity than talin in the same experiments, i.e., 100 cpm/5 μg of protein, corresponding to 0.02% of total radioactivity. Other soluble proteins such as carbonic anhydrase or ovalbumin have been shown to incorporate comparable small amounts of label upon incubation with [^{3}H]PTPC/11-containing liposomes (Harter et al., 1988). Talin in the same experiment incorporated 1570 cpm/5 μg of protein.

As shown in Figure 6 (lanes 2 and 3), the presence of 130

mM KCl and 1 mM $MgCl_2$ reduced somewhat labeling of both vinculin (to 600 ± 170 cpm/5 μg, $n = 3$) and talin (to 815 ± 410 cpm/5 μg, $n = 4$). Labeling of proteins was absolutely dependent on photolysis. Nonphotolyzed talin incorporated 0–30 cpm/5 μg of protein (Figure 6, lane 1).

When 15 μg of talin and 15 μg of vinculin were preincubated together—prior to the addition of liposomes—labeling of both proteins was not affected (Figure 6, lane 4). Talin incorporated 1270 ± 540 cpm, $n = 4$, and vinculin 900 ± 430 cpm/5 μg of protein under these conditions.

DISCUSSION

Our attempt is to reconstitute cytoskeleton membrane assembly structures (CYMAS) and to assay for the function of associated proteins. The functions of amphitropic proteins when reconstituted into protein complexes or into an environment, e.g., lipid bilayer, may differ from biochemical reactions which have been described for individual, isolated proteins in solution (Isenberg, 1991). In vitro, talin has been reported to interact with negatively charged phospholipids (Heise et al., 1991; Goldmann, 1992) and, on the other hand, to bind to actin (Muguruma et al., 1990; Goldmann & Isenberg, 1991) and to nucleate its polymerization in vitro (Kaufmann et al., 1991). In vivo, talin can frequently be colocalized with vinculin; another actin binding protein (Isenberg et al., 1982; Ruhnau & Wegner, 1988; Westmeyer et al., 1990) and lipid binding protein (Ito et al., 1983; Niggli et al., 1986). Both proteins are now widely accepted as markers for actin filament–membrane anchorage sites (Volberg et al., 1986; Draeger et al., 1989).

In a first series of experiments, we were interested if the two reported features of talin, namely, (a) nucleation of actin polymerization and (b) insertion into lipid bilayers, are maintained when vinculin is added back to the in vitro system. The experiments are not trivial, since four purified proteins, talin, vinculin, actin, and NBD–actin, have to be available at one time.

When evaluating the function of talin versus talin–vinculin complexes, the previously published overall binding constants are of importance; for talin–actin binding a K_d of $\sim 0.3 \times 10^{-6}$ M has been measured (Goldmann & Isenberg, 1991), which is a low-affinity interaction. For the interaction of talin to vinculin, Burridge and Mangeat (1984) determined a K_d of approximately 2×10^{-8} M and a stoichiometry of 3:1. Since the binding is most likely tighter than previously reported (Burridge, personal communication), the affinity of talin for vinculin appears to be 1–2 orders of magnitude higher than the affinity between talin and actin. Due to possible partial denaturation of talin, the initially reported 3:1 stoichiometry between talin and vinculin is most likely an underestimate (Burridge, personal communication). Since only one talin binding domain on the vinculin molecule and only one binding site for vinculin along the talin sequence could be mapped so far (Critchley et al., 1991), a 1:1 stoichiometry for vinculin–talin interaction is more likely. To account for this assumption, we have in our assays preincubated talin with vinculin at a molar ratio of 1:1, which is in excess to ensure the reported 3:1 stoichiometry and is sufficient to form a 1:1 complex.

A ternary complex of talin, vinculin, and actin is actually formed as demonstrated by scanning calorimetric analysis of all possible interactions between the three protein species. The precise stoichiometry within the ternary complex (vinculin–talin–actin) consisting of low- and high-affinity binding sites is not easy to obtain with the currently available techniques; most of these contain centrifugation steps by which weak binding forces are disrupted (one of the reasons why talin–actin binding was difficult to demonstrate at all). The use of Foerster-transfer assays of differently labeled proteins are currently under way to address this problem.

In this study, the actin nucleation assays are based on the low-affinity interaction between talin and actin. We have shown in Tables I–III that the overall binding constants for talin–actin and the nucleation rate constants for polymerization are similar when compared with conditions where vinculin–talin–actin complexes do form. Since we do not anticipate that a low-affinity interaction dramatically changes high-affinity binding of preincubated talin–vinculin complexes, there are good reasons to assume that the K_d and stoichiometry determined for talin–vinculin is similar within the ternary complex formed between preformed talin–vinculin complexes and actin monomers.

We have shown that the polymerization rate constants for G-actin only increase in the presence of talin and that this increase occurs independent of the presence of vinculin (table III). It is of interest that the polymerization rate constants of actin and actin–vinculin in the presence and absence of talin differ inversely with temperature. It is, however, not yet clear whether this is due to a conformational change within the protein complex or is induced by talin itself.

By applying a photoactivatable lipid analogue [^{3}H]PTPC/11, which selectively reacts with hydrophobic membrane-embedded domains of proteins, we have been able to show that talin, like vinculin, partially inserts into the hydrophobic part of negatively charged liposomal bilayers. This insertion, as judged by labeling intensity, occurs in a similar manner irrespective of whether talin is preincubated with vinculin to form a talin–vinculin complex or not. This finding is by no means unimportant. Further investigation is necessary before we can demonstrate that the talin–vinculin complex—as such—still exists after reconstituting into the bilayer. Experiments are in progress to clarify this point of interest.

So far, our data present evidence that two important functions of talin, namely, (a) actin filament nucleation and (b) membrane insertion, are still valid when talin is complexed with vinculin.

ACKNOWLEDGMENT

We gratefully acknowledge the donation of [^{3}H]PTPC/11 by Dr. J. Brunner (ETH, Zürich). We acknowledge the excellent technical assistance of K. Mujynya and Ms. H. Kirpal as well as the support from Dr. E. Sackmann. We also thank Ms Liz Nicholson (MA) for careful reading of this manuscript.

REFERENCES

Beckerle, M. C., & Yeh, R. K. (1990) *Cell Motil. Cytoskeleton 16*, 7–13.

Bradford, M. (1976) *Anal. Biochem. 72*, 248–254.

Brunner, J. (1989) *Methods Enzymol. 172*, 628–687.

Brunner, J., Spiess, M., Aggeler, R., Huber, P., & Semenza, G. (1983) *Biochemistry 22*, 3812–3820.

Burridge, K., & Mangeat, P. (1984) *Nature (London) 308*, 744–746.

Burridge, K., Fath, K., Kelly, T., Nuckolls, G., & Turner, C. (1988) *Annu. Rev. Cell Biol. 4*, 487–525.

Chamberlain, J. P. (1979) *Anal. Biochem. 948*, 132–135.

Collier, N. C., & Wang, K. (1982) *FEBS Lett. 143*, 205–210.

Critchley, D. R., Gilmore, A., Hemmings, L., Jackson, P., McGregor, A., Ohanian, V., Patel, B., Waites, G., & Wood, C. (1991) *Biochem. Soc. Trans. 19*, 1028–1033.

De Pasquale, J. A., & Izzard, C. S. (1991) *J. Cell Biol. 113*, 1351–1359.
Detmers, P., Weber, A., Elzinga, M., & Stephens, R. E. (1981) *J. Biol. Chem. 256*, 99–104.
Draeger, A., Stelzer, E. H., Herzog, M., & Small, J. V. (1989) *J. Cell Sci. 94*, 703–711.
Feltkamp, C. A., Pijnenburg, M. A. P., & Roos, E. (1991) *J. Cell Sci. 100*, 579–587.
Geiger, B., Volk, T., Volberg, T., & Bendori, R. (1987) *J. Cell Sci. Suppl. 8*, 251–272.
Goldmann, W. H. (1992) *Biochem. Soc. Trans. 20*, 121S.
Goldmann, W. H., & Isenberg, G. (1991) *Biochem. Biophys. Res. Commun. 178*, 718–723.
Goldmann, W. H., & Isenberg, G. (1992) *Biochem. Soc. Trans. 20*, 273S.
Goldmann, W. H., Kaufmann, S., & Isenberg, G. (1991) *Biochem. Soc. Trans. 20*, 50S.
Harter, C., Bächi, T., Semenza, G., & Brunner, J. (1988) *Biochemistry 27*, 1856–1864.
Heise, H., Bayerl, T., Isenberg, G., & Sackmann, E. (1991) *Biochim. Biophys. Acta 1061*, 121–131.
Hock, R. S., Sanger, J. M., & Sanger, J. W. (1989) *Cell Motil. Cytoskeleton 14*, 271–287.
Isenberg, G. (1991) *J. Muscle Res. Cell Motil. 12*, 136–144.
Isenberg, G., Leonard, K., & Jockusch, B. M. (1982) *J. Mol. Biol. 158*, 231–249.
Ito, S., Werth, D. K., Richert, N. D., & Pastan, I. (1983) *J. Biol. Chem. 258*, 14626–14631.
Izzard, C. S. (1988) *Cell Motil. Cytoskeleton 10*, 137–142.
Kaufmann, S., Piekenbrock, T., Goldmann, W. H., Bärmann, M., & Isenberg, G. (1991) *FEBS Lett. 284*, 187–191.
Laemmli, U. K. (1970) *Nature (London) 227*, 680–685.
Laskey, R. A., & Mills, A. D. (1975) *Eur. J. Biochem. 56*, 335–341.
Lowry, O. H., Rosebrough, N. J., Farr, A. L., & Randall, R. J. (1951) *J. Biol. Chem. 193*, 265–275.
MacLean-Fletcher, S., & Pollard, T. D. (1980) *Biochem. Biophys. Res. Commun. 96*, 18–27.
Muguruma, M., Matsumura, S., & Fukazawa, T. (1990) *Biochem. Biophys. Res. Commun. 171*, 1217–1223.
Niggli, V., Dimitrov, D. P., Brunner, J., & Burger, M. M. (1986) *J. Biol. Chem. 261*, 6912–6918.
O'Halloran, T., Molony, L., & Burridge, K. (1986) *Methods Enzymol. 134*, 69–77.
Ross, P. D., & Subramanian, S. (1981) *Biochemistry 20*, 3096–3102.
Ruhnau, K., & Wegner, A. (1988) *FEBS Lett. 228*, 105–108.
Spudich, J. A., & Watt, S. (1971) *J. Biol. Chem. 246*, 4866–4871.
Turner, C. E., & Burridge, K. (1991) *Curr. Opin. Cell Biol. 3*, 849–853.
Volberg, T., Sabanay, H., & Geiger, B. (1986) *Differentiation 32*, 34–43.
Westmeyer, A., Ruhnau, K., Wegner, A., & Jockusch, B. M. (1990) *EMBO J. 9*, 2071–2078.